Centrally Pivoted Tilting Pad Thrust Bearing with Carbon Based Coated Collar - Experimental Results of Low and Medium Speed Operation

INTRODUCTION

According to the classical Reynolds equation, an important condition of generating film pressure in a bearing is the existence of convergent oil gap, which seems impossible in thrust bearings with centrally pivoted pads [1]. In practice however, centrally pivoted pads are in use in cases where bi-directional operation is required (e.g. in hydro-generators of pumped storage power plants). The research results show, that the load carrying capacity existing in these cases is due to deformations and irregularities of shape (pad surface waviness, collar run-out, etc.) [2] [4]. Experimental research has proved that these bearings operate at higher temperature [5], smaller film thickness and greater losses than the bearings with off-set pivoted pads [6]. Theoretical works focused on investigation of thrust bearing with centrally pivoted pads are extremely rare. One of the example is work of Fillon et al [7] who presented theoretical analysis of the influence of pad active surface profile, including long chamfers, on the properties of PTFE-faced pad. Irrespective of pad pivot position, a well recognized limitation of tilting pad thrust bearings is low load carrying capacity at transient states, especially during start ups and stops. A sliding speed of the order of meters per second is required for a reliable operation of these bearings under considerable axial loads. Limits of operation of hydrodynamic thrust bearing were summarized in a work of Leopard [8]. It was pointed out, that the limits of operation both, minimum film thickness for relatively low speed bearings and temperature for high speed applications, depend significantly on the bearing pad lining material. In industrial practice, manufacturers of the most common babbitted bearings declare a safe operation starting from sliding speed of approximately

3 m/s, being the equivalent of 100-500 rpm, with lower rotational speed possible for larger bearings [9]. When a bearing is used in the operational conditions close to the limit, it is important to realize the margin of its safe operation, and it seems to the authors, that this can be reliably specified only by experimental testing of a particular bearing in particular operating conditions. Reports of such investigations are however rare.

De Guerin et al. in [10] and [11] presented the results of experimental testing of a 660 mm (26 inch) thrust bearing in which bearing seizure load was evaluated for different shaft speeds changed in the range of 500-3000 rpm and different levels of lubricant flow. One of the interesting findings was, that a full eight pad bearing failed at much lower specific load than a two pad bearing. Explanation of this phenomena can be found in the paper by Neal [12], who investigated experimentally the influence of pad number on bearing performance. He observed that reduction of pad number lowered runner and bearing temperatures which in consequence led to the increase of bearing margin of safety.

Yamada et al. [13] presented results of destructive tests of a tilting pad thrust bearing (OD 200 mm) with the pads lined with PEEK. The seizure of a bearing at 1000 rpm occurred at the specific load of 26 MPa. Gardner [14] presented results of failure tests for six-inch thrust bearing and different pads and alloy materials at high speed conditions (6000 rpm). It was noticed that the load of bearing failure depended significantly on runner sliding surface finish. Higher loads were acceptable in case of better surface finish. Depending on pad material the first symptom of bearing failure (rapid temperature increase) was observed for bearing specific load equal to 11-15 MPa. Operational low speed limit (minimum film thickness) of a large uni-directional thrust bearing of OD=1173 mm was experimentally studied by Brown et al. [15]. Three configurations of the bearing with different pad number and the distribution of the springs supporting the pad were tested. It was found that hydrodynamic action of the bearing was possible at the speeds of

10-20 rpm (sliding speed of 0.48 – 0.96 m/s). The friction coefficient at the transition between fluid film and mixed lubrication was equal to 0.0004 – 0.0006, depending on the bearing and pad support spring mattress configuration.

A separate class of researches reported in the literature is bearing behaviour during start – stop period of operation. Especially the large thrust bearings of hydrogenerators are prone to failures at these regimes, because of excessive pads thermal deformations [16] and [17]. A well known method of improving the reliability of large thrust bearings in transient states is applying the systems of hydrostatic jacking. Another method is heating the oil in the bearing housing in order to decrease pad deformation due to decreased thermal gradient across the pad thickness [18]. A detailed experimental study of phenomena occurring during start-up of a 584 mm bearing under the specific load of 5 MPa was presented by Gustafson [19]. He found that the hydrodynamic action starts just after several degrees of shaft rotation. Time of load application to a bearing in standstill before start of rotation during tests did not change significantly the break-away torque. Recent paper on experimental investigation of start-stop of tilting pad thrust bearing was published by Li et al [20]. It contained the results of the measurements of temperatures and film thickness during start-stop cycles in a tilting pad bearing equipped with the equalizing load distribution mechanism. The results with large discrepancy of the pad temperatures reaching over 12°C in particular pads demonstrate limited efficiency of the equalizing mechanism. This was also reported in the paper of Gustafson [19]. The friction torque during start up of a journal and thrust bearing was also studied experimentally by Bouyer et al. [21] and [22]. The research comprised the influence of load, bearing dimensions and material of the bearing lining. It was observed that the breakaway torque at the start up was much smaller in the bearing lined with PEEK than in the case of babbitted bearing. Such results were confirmed also in the tests on small specimen carried out by Golchin et al. [23].

OBJECTIVE OF THE RESEARCH

Literature search showed, that there were only few researches in which tilting-pad bearings were tested at low speed. This was probably because low speed operation is an unusual operating condition for fluid film bearings. In case of low relative sliding speed, oil film thickness is likely be too small to avoid direct contact of operating surfaces – taking into account surfaces imperfectness, as waviness, roughness or non parallelism. Fluid friction in bearings can then change to mixed friction, which increases bearing losses, oil and bearing temperature and intensifies wear of sliding surfaces. There is a risk, that bearing operating in the conditions of mixed friction for a longer time will fail. Research and calculations are meant to help understanding bearing behavior in severe operating conditions, therefore they are important for improving reliability of the bearing performance, e.g. close to the transition to mixed friction regime or during transient states of its operation.

Objective of the research was to study phenomena accompanying the prolonged operation of a tilting-pad thrust bearing in the conditions of low speed and high load. Experimental research of two eight pad thrust bearings made of steel with symmetrical support operating against the collar coated with a carbon based coating with a special layering was carried out. Bearing performance was checked experimentally in several steady state tests at relatively low speed conditions. For the purpose of comparison, a couple of high speed tests were also carried out, in order to observe the differences in bearing performance operating in different conditions. Series of start-stop cycles were also carried out to study the behaviour of a bearing with centrally supported pads under transient states of operation. Additionally, Stribeck curve was reproduced experimentally for the tested bearings. This allowed to determine the conditions at which transition between fluid and mixed friction was occurring.

RESEARCH FACILITY

Test rig installed at the Laboratory at Gdansk University of Technology was used for experimental investigation of bearings performance. Main components of the test rig are: test bearing, driving system and hydraulic system for lubrication and loading of thrust bearings. Test stand general view and bearing housing cross section are presented in Fig. 1.

There are two thrust bearings placed in the test stand housing (5) - front bearing (1) and back bearing (3), mounted against a thrust collar (2) fixed to the shaft. Axial force of up to 90 kN is exerted by a ring shaped hydraulic piston (4). The front bearing is mounted to the plate (6) supported on a spring structure of a special torque meter (7). Operating conditions of the tested bearings are within the range met in the industrial bearings - with specific loads up to even 10 MPa (depending on test bearing area) and sliding speeds up to 35 m/s. The driving motor of 30 kW power and 3000 rpm of nominal speed is controlled by a frequency converter. The range of operational speeds was adjusted to the planned research by a newly built timing gear transmission which can be installed as multiplicating or reducing transmission, by swapping the pulleys, so that maintaining low rotational speed of the shaft at a stable level of about 25 rpm was possible. Due to recent redesign of the lubricating system, different methods of cold oil supply can be tested. Bearing housing and oil supply system design allows one to adjust the level of oil in the housing starting from fully flooded lubrication to completely evacuated housing cavity, when directed lubrication is to be tested [24]. Maximum supply of oil in the test rig is 45 l/min for both bearings and suitable oil flow can be adjusted by sets of flow control valves and flow meters. In the reported tests oil was supplied with the flow rate of $Q_{in\ b} = Q_{in\ f} = 14.5$ l/min for each bearing (see symbols at Fig. 1 b) at the temperature of 40 ^{o}C ±0.2 ^{o}C controlled with the use of water cooler. ISO-VG 68 oil was used as a lubricant (measured oil properties: $\rho_{25} = 875$ kg/m^3,

η_{40} = 0.061 Pas, η_{80} = 0.012 Pas). Lubricating oil was filtered with 5 μm accuracy filter. The main specifications of the test rig are listed in Table 1.

The test rig is equipped with a precise torque meter shown in Fig. 2 a. The torque meter allows for measuring small friction torque **M** in the front bearing with minimum influence of large axial force **W** applied to the bearing. The idea of this device is shown in Fig. 2 b. The front bearing is fixed to the plate, which is connected in elastic way to the test rig head with the use of a special torque meter spring. Torque **M** applied to the front bearing is transferred to the test rig head through the spring, and causes small rotation of the plate with respect to the bearing housing. The angle of rotation is measured with the use of two displacement sensors fixed to the test rig head (Fig. 2 a). The result of friction torque meter calibration carried out before tests is shown in Fig. 2 c. It presents the relationship between friction torque displacement sensors readings (in μm, expressed as difference of displacement signals to improve the accuracy) and axial force **W** applied to the bearing and external torque applied **M** to the plate. Non linear behaviour of device was observed for higher values of applied torques (M > ~ 25 Nm) and axial loads (W > ~ 40 kN). It should be mentioned, that the highest values of friction torque measured during the tests were lower than 20 Nm, so distance sensors readings were recalculated into friction torque with the use of data presented in Fig. 2 c and linear interpolation. A detailed description of torque meter can be found in [25].

TEST BEARING AND INSTRUMENTATION

According to the configuration of the test rig, two tilting pad thrust bearings were operating against both sides of the collar. Test bearing pads were supported linearly on the central rib support. The pads were made of steel hardened to 45 HRC and without any bearing alloy. Sliding surfaces of the pads were grinded to Ra parameter of 0.32 μm. Sliding surfaces of the collar were

covered with a carbon based coating (Triondur®CX$^+$ [26]). This lining type was applied previously in numerous applications in order to prevent or minimize wear of the parts in contact. The friction losses in the valve trains of passenger cars were for example reduced by the factor of two using this type of coating [27]. Considering the problems of bearing operation at low speeds, application of such surfaces also in fluid film bearings seems to be a good choice. Although the rubbing surfaces are normally separated by a fluid film, with no need of anti-wear properties, during start-ups and stopping, when mixed friction occurs such a coating can prevent accelerated wear of the bearing. From the point of view of this research, it was also very important as it allowed to reduce or even eliminate collar wear, reducing the influence of gradual deterioration of collar quality on the research results. Thickness of the collar sliding layer was about 3 μm. Details of tested thrust bearing pad are shown in Fig. 3 a), while specifications of the bearing are listed in the Table 2.

Instrumentation of the bearings comprised 12 J-type thermocouples of 1 mm diameter installed in two pads of each of the test bearings (3 thermocouples in two selected pads of front and back bearing). Instrumented pads were marked with letters **A** and **B** (see Fig. 3 b).

Positions of the thermocouples were selected in order to monitor the temperature in the hottest spots close to the pad surface, as well as at the inlet area. It was also possible to evaluate the temperature gradient across pad thickness due to installation of one thermocouple (TF_B2b in front bearing) close to the bottom of the pad. During the tests temperatures in both (front and back) bearings were measured. Trends and distributions of temperature measured in bearings were very similar and the differences between respective thermocouples locations did not exceed 3 ^{o}C. For the sake of saving space, only data measured for the front bearing are presented in the paper. Positions and symbols of the temperature sensors installed on the front bearing are shown in Fig. 4 and collected in Table 3.

Mean value of film thickness at the pivot was measured with the use of one displacement sensor installed axially in the test rig plate (Fig. 1 b, Fig. 3 b). It was noticed, that zero-film level measured with the use of distance sensor depend on tightening torque of the screws used to fix the bearing plate to the housing and also on temperature. Because of this, immediately after the stop of each test (when the test stand was still hot) zero-film level for individual test was measured. This was completed by applying axial bearing force (for about 5 minutes) of the same value, as used during the completed test. Average reading of distance sensor from this measurement was used as reference film value. Mean value of the film thickness at the pivot was than recalculated as the difference between distance sensor reading recorded during bearing tests and zero-film level measured after stop.

Uncertainties of the sensors were evaluated (basing on classes of the sensors, their measuring range and additional calibrating measurements) as: ± 3 μm for distance sensor, ± 0.8 ^{o}C for thermocouples and ± 0.3 Nm for friction torque meter.

TEST CONDITIONS

Test conditions were specified so as to combine the requirements of the potential applications and the limitations of the test rig (Table 4). In general the research plan comprised 6 tests at steady conditions with different loads and speeds. The duration of the steady state tests was 10 hours, apart from both tests with rotational speed equal to 1000 rpm which lasted 5 hours each and the test at high specific load (10 MPa) and low speed (100 rpm) which lasted 20 hours. After steady state tests, 100 start-stop tests were carried out. In each start-stop cycle, according to the planned procedure, shaft was accelerated to 500 rpm in ~40 s without load and then the load was increased starting from 0 kN to 80 kN in ~35 s (such conditions were obtained in about 1 minute and 15 seconds from the start of the test). Bearings were operated under such conditions for

about 3 minutes, and then shaft speed was decreased under load to zero (in about 1 minute). One start-stop test comprised about 5 minutes.

Bearing inspection after start-stop tests did not show any signs of the wear of the collar lined with the carbon based coating, but on the sliding surface of the steel pads some slight areas of wear were observed. On this basis, it was decided to study the transition to mixed friction as an ultimate limit of bearing load carrying capacity. According to the theory of fluid film bearings, the coefficient of friction decreases with increased bearing load and finally reaches its minimum just before the transition to the mixed lubrication regime. This phenomenon is illustrated by the Stribeck curve, which presents relationship between bearing coefficient of friction and dimensionless load parameter (Hersey Number, Hs), being a function of: load, oil viscosity and speed. Transition to mixed friction tests were carried out with a constant specific load (in two series at 2.5 MPa and 5 MPa) and a gradually decreased speed, from 120 rpm to 20 rpm (for 2.5 MPa) and to 25 rpm (for 5 MPa). The first evidence of increasing torque or temperature indicates conditions of transition between fluid film and mixed friction expressed in this work in the terms of Hersey Number. Hersey Number values were evaluated, for each level of bearing operational parameters (W, n), with the use of dynamic viscosity at the temperature equal to maximum temperature of the tests bearing pad - viscosity as a function of temperature calculated applying a commonly used Sutherland's formula for liquids.

RESULTS

Steady state tests were carried out according to the plan presented in Table 4. The sequence of the tests was planned so as to move gradually from easier to more severe operating conditions. During steady state tests, after reaching thermal equilibrium conditions (which took 0.5-1 hour) all measured parameters were very stable, without any significant changes throughout the whole

load/speed step. That is why, in further parts of the paper only mean values of measured parameters are presented. The results of steady state tests are collected in Table *5* and in the following graphs.

The highest measured temperature of the front bearing (thermocouples TF_A2 or TF_B2 at the pad outlet, see Fig. 4) in the subsequent steady state tests is shown in Fig. 5. It can be observed, that the maximum bearing temperature was rising as the speed and load were increased, despite of test at 100 rpm and 10 MPa, where the increase of specific load from 5 MPa to 10 MPa caused the decrease of temperature. This inconsistency was due to the fact, that the highest specific load (10 MPa) was obtained by reducing number of bearing pads from eight to four. Similar method of increasing bearing specific pressure in experiments was also used by Harika et al. [28]. This introduced changes in thermal behaviour of the bearing - improved efficiency of cool oil supply to the pad inlet, most likely caused the decrease of collar temperature, and finally resulted in lower pad temperatures [12]. Effect of the doubled axial bearing load on measured maximum temperature can be observed for two bearing speeds: 100 rpm and 1000 rpm. Quite large temperature increase was measured for the highest bearing speed (~4.9 ^{o}C), and very low for low bearing speed (~0.7 ^{o}C). Inconsistency of the result trends was also noticed for the measured friction torque values (decrease of torque with the increase of specific load), as shown in

Fig. 6 a. This was caused by reduction of pad number and oil shearing losses. Based on the friction torque the coefficient of friction in the bearing can be evaluated with the use of equation [1]:

$$\mu = \frac{M}{W \cdot r_m} \qquad [1]$$

where W was equal to 35.8 kN (for p = 2.5 MPa) or 71.6 kN (for p = 5 and 10 MPa) and r_m (mean bearing radius) was equal to 0.0675 m. The result of friction coefficient is plotted in Fig. 6 b. As one would expect based on the theory of hydrodynamic lubrication, coefficient of friction decreases with increasing bearing load. In Fig. 6 b, the smallest value of 0.0014 (for 100 rpm and 10MPa) is almost five times smaller than its maximum value of 0.0069 (for 3000 rpm and 2.5 MPa). It should be however noted, that in case of full eight pad bearing at 10 MPa and 100 rpm, measured value of friction torque would have been higher, due to increased surface at which oil is sheared.

Changes of the mean film thickness over the bearing support are illustrated in Fig. 7. Hydrodynamic film thickness also decreases with an increased bearing load. The smallest value of 6.6 μm was obtained for 100 rpm and 10MPa, while the maximum value of 37.6 μm was evaluated for the speed of 3000 rpm and specific load of 2.5 MPa.

It is also interesting to compare the temperature distribution on the bearing pad for different operating conditions. For Test I (Fig. 8 a), when the bearing was operated at 3000 rpm one can observe a distinct difference between temperature at the inlet and in the outlet area exceeding 15°C, very characteristic for fluid film bearings. Quite contrary, in the test at 100 rpm and 10 MPa the difference was only 0.1°C (Fig. 8 b). Probably it is an evidence of almost parallel operation of the pad for smaller speeds without tilting, which is observed only at higher speeds - traces on the pads found close to the leading edge seem to confirm this opinion.

For a test bearing one can specify the value of allowable film thickness (e.g. based on DIN 31654 [29] or ISO 12130 [30] - it should, however be mentioned that both the standards should not be used for symmetrically supported tilting pad bearings). For the size and roughness of the test bearing, the allowable film thickness is equal to about 5 μm. It is not easy to judge whether the values obtained from measurements were above the limit - especially 6.6 μm of the mean film

thickness over the pad support (for the most severe Test VI - 10 MPa, 100 rpm) is close to the allowable value of minimum film thickness. Even with small pad tilting the minimum located close to the trailing edge might have been smaller than the recommended allowable film thickness.

START STOP TESTS

The start stop tests were performed in the range of 0-500 rpm with the load of 80 kN (p = 5.6 MPa) applied immediately after reaching the nominal speed and stopping under load. Changes of the temperatures during one cycle are shown in Fig. 9 - one can see an increase of temperatures by about 10°C, the bearing temperature started to rise only after the load was applied, at the earlier phase of speed increase and no load the temperature dropped by 1-2°C. This temperature drop during rump up with no load was caused by rapid increase of the oil film thickness and cooling effect of intensive oil flow (Fig. 10 a). The temperature measured in the pad was very evenly distributed - the differences in particular sensor locations did not exceed 1°C. It should be noted, that the time in which bearing load and rotational speed were kept constant was too short to obtain thermal equilibrium conditions. Bearing temperatures and oil outlet temperature did not reach the equilibrium conditions, as it can be observed in Fig. 9. Then, during the slow down phase bearing temperatures decreased as the shaft speed was decreasing. After the stop of the shaft, temperature decrease graph changed its slope, due to the contact between pads and collar.

Changes of the friction torque and mean film thickness over the bearing support during one selected start/stop cycle are shown in Fig. 10 a. One can observe that the film thickness reaches almost 70 μm at no load conditions, about 17 μm during constant speed phase of the test and

drops to about 2-4 μm during the stopping phase. The friction torque was equal to approximately 15.6-16.0 Nm then, in the slow down phase of the cycle it was decreasing reaching minimum of about 6.4-7.0 Nm. Finally it increased rapidly as the friction mode was changing from a full film lubrication to mixed friction. Transition from full film to mixed friction was observed at about 35-45 rpm just after 628.9 minute of the test in Fig. 10 b. The increased torque caused the stop of the shaft, because of sliding in the multi-disc friction clutch of the test facility - this can also be observed in Fig. 10 b as a faster decrease of rotational speed. The peak value of the torque is the result of dynamic load of the torquemeter caused by rapid shaft deceleration and it is not directly connected to tribological phenomena. Before shaft stop, distance sensor readings showed "wavy" course (Fig. 10 b). This was caused by magnetic irregularity of target surface and collar sliding surface geometrical irregularities (flatness and waviness) and its axial run-out, which were measured in separate measurements and found to be equal ~ 3 μm. Transition to mixed friction occurring at 35-45 rpm, allows to evaluate Hersey Number of the bearing at transition. Additional data required to such a calculation was: temperature equal to about 49°C (taken from Fig. 9), which yields dynamic viscosity of 0.0402 [Pa s], specific load p = 5.58 MPa (F = 80 kN). Then Hersey Number is equal to 4.8×10^{-9}.

During the start-stop tests, the parameters observed in each cycle were changing slightly - these changes were plotted in the following graphs as a function of cycle number. Maximum temperature of the pads are shown in Fig. 11. Quite a distinct change occurred after about 45 cycles - maximum bearing temperatures dropped (even by about 0.5°C in a back bearing). Minimum torque observed at the slow-down phase just before the stopping of the shaft (Fig. 12 a) decreased continuously to the 45th cycle of start stop tests by almost 0.5 Nm. For next cycles it was almost constant at the level of 6.5 – 6.6 Nm, and occurred at a slightly lower rotational speed (Fig. 12 b). It is probably the effect of running in of the bearing, especially as new "polishing"

marks were observed after start-stop tests. The friction torque in the steady state phase (at 500 rpm and 80 kN) did not change significantly during the course of start-stop tests.
It is worth noticing that after start-stop tests the area of wear marks (in the form of polishing the pad surface) increased, but still those marks were limited to specific locations only: limited spots located either close to the leading edge, at the outer periphery or (in one pad only) close to the trailing edge. These marks are another evidence of almost parallel operation of the pad with very low film thickness and mixed friction during the last phase of stopping. The polishing traces were not easy to document by taking photographs so it was decided to outline them with the use of a marker to show their extent and compare their development after each stage of the tests. An example of the pattern of polishing marks on the pads is shown in Fig. 13. No visible wear marks were observed on the collar surface covered with DLC-type coating. The collar roughness measured between the tests was gradually decreasing - Ra parameter changed from 0.6 μm to 0.45 μm.

TRANSITION TO MIXED FRICTION PARAMETERS - STRIBECK CURVE REPRODUCTION

In Fig. 14 a the most classical Stribeck curve showing the friction coefficient as a function of dimensionless load parameter - Hersey Number is plotted. Hersey Number was evaluated at each point with the use of current bearing temperature and appropriate value of oil viscosity evaluated on the basis of own measurements of the viscosity of the particular oil used in the tests. Quite a clear beginning of the transition to mixed friction in the plot for 5 MPa (black line) can be observed, while it seems that the speed was still too high for a bearing operating under a specific load of 2.5 MPa (grey line). Measured value of the minimum friction coefficient was equal to

0.00125 (M = 6,06 Nm, n = 25,2 rpm, p = 5 MPa). Unfortunately it was impossible to maintain a constant rotational speed at a lower level. In the Fig. 14 b it is shown that for the lowest tested speed, the film over the supporting edge was very thin (3 μm at 5 MPa and 5 μm for 2.5 MPa). A real value of the minimum film thickness (not the mean film over the pad support) is lower, which shows that a transition to mixed friction in which the contact between the pad and the collar occurs was very close.

Temperature measurements for specific bearing pressure equal to 5 MPa (see Fig. 15) show a temperature rise for smaller values of Hersey Number, clearly visible especially for the back bearing (TB_A2, TB_B2). This is another evidence of transition between fluid and mixed lubrication for shaft speed ~30 - 33 rpm. In the front bearing due to slightly different conditions of operation in comparison to the back bearing (heat transfer, arrangements for lubricating oil flow, etc.), transition between fluid and mixed lubrication can be observed for slightly lower values of shaft speed (~25 rpm). Hersey Number at which transition in the test bearing occurred can be estimated as $5.5 - 6.1 \times 10^{-9}$.

DISCUSSION OF THE RESULTS

Tests of the bearing with material selection - collar lined with carbon based coating and steel pads with symmetrical pad support were carried out at severe operating conditions - low speed, high specific load. The conditions were beyond standard operating conditions of the tilting pad thrust bearings. In case of tests with 100 rpm, sliding velocity at mean bearing radius was equal to only ~0.7 m/s. Moreover a series of 105 start-stop cycles with stops under load were performed. In these conditions bearing was operating very well with minimum signs of the contact on pad surfaces (in the form of surface polishing) and no visible traces on the collar surface (just changes in roughness). Tests in transition from fluid to mixed friction were also performed for tested bearing.

In cases where bearings operated under conditions of low speed, very low temperatures were measured, compared to cases of 1000 rpm and 3000 rpm. Additionally, temperature measured in the pad had a very uniform distribution, which differed from the case of high speed tests. This was due to less intensive oil shearing in the oil gap, which is proportional to the bearing sliding speed and also due to the pad tilt. Uniform temperature distribution in case of low speed tests probably means, that the pad had only small inclination and its surface was almost parallel to the collar. Parallel position of the pad with respect to the collar was also indirectly confirmed by the traces on contact observed on the pad surface, but on the other hand one should also note that the differences are so small that they are within the uncertainty range of the temperature measurement.

In low speed conditions, bearings operated with lower friction torque compared to high speed case. The increase of speed by a factor of 10 (from 100 rpm to 1000 rpm) caused the increase of the friction torque only by a factor of 2. It should be pointed out, that under low speed conditions oil temperature in the oil gap is lower, which results in higher oil shear stresses due to larger oil viscosity. Additionally, the uniform distribution of the pad temperature did not allow to generate thermal deflection of the sliding surface, which can help to obtain convergent oil gap, especially in case of symmetrical support. Probably these two effects influence the proportion between losses for low and high speed cases.

Coefficient of friction decreased by a factor of five - from 0.0069 (for 3000 rpm and 2.5 MPa) to 0.0014 (for 100 rpm and 10 MPa) as the bearing load was increasing. The mean film thickness (over the support) decreased down to 6.6 μm and 3-4 μm in the testing of the transition to mixed friction.

Results of start-stop tests show that tested bearing can operate successfully in the conditions of transient state operation. Measured parameters trends were very repeatable compared to the

results measured at individual start-stop cycles. Changes in measured trends of maximum temperatures and minimum friction torque before shaft stop for successive individual cycles showed typical running-in process, starting with more intensive losses (higher bearing temperatures, higher friction torques) and decreasing to lower values after reaching run-in conditions. After 45th cycle, all bearing parameters controlled during start-stop tests ceased to change. Probably, the initial phase of bearing running-in process resulted also in new polishing marks visible after tests on pads sliding surfaces.

Tests in transition to mixed friction proved, that bearing with symmetrically supported pads can operate under hydrodynamic friction at relatively low speed. Transition between fluid and mixed friction was clearly visible in tests carried out at 5 MPa. The evidence was the increase of the measured temperature with the decrease of the shaft speed was the result of increased bearing losses (higher coefficient of friction). During start-stop tests the transition was observed as a rapid increase of the torque. Hersey Number at the transition was similar in both cases and equal to, respectively 5.5 - 6.1 x 10^{-9} and 4.8 x 10^{-9}.

Results of the tests proved, that tested tilting-pad thrust bearing with symmetrical support can operate successfully in the conditions of relatively high load and low sliding speed. No significant wear signs were observed on both pad and collar sliding surfaces after completing the whole test program, including long-lasting steady state, start-stops and transition to mixed friction tests.

MAIN CONCLUSIONS

Summarizing the described research, the following main conclusions can be formulated:

- tested tilting pad thrust bearing with symmetrical support operating against collar covered with carbon based coating was able to operate successfully beyond usual technical range of operation of hydrodynamic bearings,

- transition between hydrodynamic and mixed friction was identified for tested bearing,
- no signs of wear were noticed on carbon based coating of the collar, even after mixed lubrication regimes and start-stop tests.

ACKNOWLEDGEMENTS

The authors from the Gdansk University of Technology wish to thank Schaeffler Technologies GmbH & Co. KG for their permission to publish and present the results.

NOMENCLATURE

n	[1/s] or [rpm]	shaft speed
p	[Pa] or [MPa]	specific pressure
W	[N] or [kN]	axial load
TF_A1, TF_A2, TF_A3, TF_B1, TF_B2, TF_B2b	[°C]	bearing temperature in locations described in Fig. 4 and Table 3
T_{in}	[°C]	temperature of the oil at the inlet to the test head
T_{out}	[°C]	temperature of the oil at the outlet from the test head
h	[μm]	mean film thickness over the pad support
M	[Nm]	friction torque in the front bearing
r_m	[m]	mean radius of the bearing
μ	[-]	friction coefficient
η	[Pa s]	dynamic oil viscosity

REFERENCES

[1] Raimondi, A.A., Boyd, J. (1955), "Applying Bearing Theory to the Analysis and Design of Pad-Type Bearings", Trans. of the ASME, **77**, pp 287-309,

[2] Raimondi, A.A., Boyd, J. (1955), "The Influence of Surface Profile on the Load Capacity of Thrust Bearings With Centrally Pivoted Pads", Trans. of the ASME, **77**, pp 321-330,

[3] Lebeck, A.O. (1987), "Parallel Sliding Load Support in the Mixed Friction Regime. Part 1 – The Experimental Data", Trans. of the ASME, J. Tribology, **109**, 1, pp. 189-195,

[4] Lebeck, A.O. (1987), "Parallel Sliding Load Support in the Mixed Friction Regime. Part 2 – Evaluation of the Mechanisms", Trans. of the ASME, J. Tribology, **109**, 1, pp. 196-205,

[5] Gardner, W.W. (1988), "Tilting Pad Thrust Bearing Tests – Influence of Pivot Location", Trans. of the ASME, J. Tribology, **110**, 4, pp. 609-613,

[6] Neal P.B., Soliman M.A.M. (1982), "The Influence of Pivot Location on the Performance of Tilting-Pad Thrust Bearings", proc. of Institute of Mechanical Engineering Seminar on Plain Bearings – Energy, Efficiency and Design, 10.11.1992 London, pp. 45-50,

[7] Fillon M., Glavatskih S.B. (2008), "PTFE-Faced Center Pivot Thrust Pad Bearings: Factors Affecting TEHD Performance", Tribology International, 41, pp. 1219-1225,

[8] Leopard, A.J. (1975), "Tilting Pad Bearings – Limits of Operation", paper no AT 385/75, *Proc. of ASLE 30th Annual Meeting*, Atlanta, pp. 1-11,

[9] "Equilizing Thrust Bearings - comprehensive design guide". Kingsbury, Inc.

[10] de Guerin, D., Hall, L.F. (1957), "An Experimental Comparison Between Three Types of Heavy Duty Thrust Bearing", Paper 79, *Conference on Lubrication and Wear*, I.M.E., London, pp. 128-134,

[11] de Guerin, D., Hall, L.F. (1957), "Some Characteristics of Conventional Tilting-Pad Thrust Bearings", Paper 82, *Conference on Lubrication and Wear*, I.M.E., London, pp. 142-146,

[12] Neal P.B. (1980), "Some Factors Influencing the Operating Temperature of Pad Thrust Bearings", Proc. of 6th Leeds-Lyon Symposium, pp. 137-142,

[13] Yamada, Y., Uesato, M., Tanaka, M (2004), „The tribological performance of PEEK lining material", paper B, *Proc. of EdF-LMS Workshop: Improvement of bearing performance under severe operating conditions*, Poitiers, pp. 1-8,

[14] Gardner, W.W. (1975), „Performance Tests on Six-Inch Tilting Pad Thrust Bearing", Trans. of the ASME, J. Lubr. Technol., **97**, 3, pp. 430-436,

[15] Brown, A.L., Medley, J.B., Ferguson, J.H. (2000), "Spring-Supported Thrust Bearings Used in Hydroelectric Generators: Limit of Hydrodynamic Lubrication", Tribology Series, **38**, pp. 261-274,

[16] Ettles, C.M., Seyler, J., Bottenschein, M. (2003), "Some Effects of Start-Up and Shut-Down on Thrust Bearings Assemblies in Hydro-Generators", Trans. of the, J. Tribology, **125**, 4, pp. 824-832,

[17] Chambers, W.S., Mikula, A.M. (1987), "Operational Data for a Large Vertical Thrust Bearing in a Pumped Storage Application", Tribology Transactions, **31**, 1, pp. 61-65,

[18] Pistner, A.E., (1996), "Some Effects of Start-Up Transient Loads on Shoe Bearings for Large Hydraulic Pump/Turbines", Tribology Transactions, **39**, 1, pp. 93-98,

[19] Gustafson, R.E. (1967), "Behavior of a Pivoted-Pad Thrust Bearing During Start-Up", Trans. of the ASME, J. Lubr. Technol., **89** 2, pp.134-142,

[20] Li, P., Yongsheng, Z., Youyun, Z., Zhao, C., Yuping, Y., 2013, "Experimental Study of the Transient Thermal Effect and the Oil Film Thickness of the Equalizing Thrust Bearing in the Process of Start-Stop With Load", Proc. of the Institution of Mechanical Engineers, Part J, **227** 1, pp. 26-33,

[21] Bouyer, J., Fillon, M. (2011), "Experimental measurement of the friction torque on hydrodynamic plain journal bearings during start-up", Tribology International, **44**, pp. 772-781,

[22] Bouyer, J., Hanahashi, M., Fillon, M., Fujita, M. (2012), "Experimental investigation of the influence of materials on the behavior of a hydrodynamic tilting-pad thrust bearing", paper no 153, *Proc. of 15th Nordic Symposium on Tribology*, Trondheim, pp. 1-5,

[23] Golchin, A., Simmons, G.F., Glavatskih, S.B. (2012), "Break-Away Friction of PTFE Materials in Lubricated Conditions", Tribology International, **48**, pp. 54-62,

[24] Rotta G., Wasilczuk M., Wodtke M. (2011), "Experimental Study Of Different Supply Designs In Hydrodynamic Thrust Bearings", paper , Proc. of EdF /Pprime Workshop: Condition Monitoring, Performance Improvement and Safe Operation of Bearings, Poitiers, p. 1-7,

[25] Dąbrowski L., Wasilczuk M. (1995), "A Method of Friction Torque Measurement for a Hydrodynamic Thrust Bearing", Trans. of ASME, J. Tribology, **117,** 3, pp. 674-678,

[26] Triondur® - technical information from: http://www.schaeffler.com/remotemedien/media/_shared_media/08_media_library/01_publications/schaeffler_2/tpi/downloads_8/tpi115_de_en.pdf, downloaded 13.04.2013,

[27] Musayev Y., Hosenfeldt T.: Triondur® Coatings as a design element for highly stressed engine components. Hauzer Conference "Environment Protection by Plasma Coating Technology" 29.03.2012, Venlo Holland,

[28] Harika E., Bouyer J., Fillon M., Mathieu H. (2013), "Effects of Water Contamination of Lubricants on Hydrodynamic Lubrication: Rheological and Thermal Modeling", Trans. of the ASME, J. Tribology, **135**, 4, pp. 1-10,

[29] DIN 31 654 standard (1991), "Hydrodynamische Axial-Gleitlager im stationaren Betrieb", Part 1-3,

[30] ISO 12130 standard (2001), "Plain Bearings - Hydrodynamic Plain Tilting Pad Thrust Bearings under Steady-State Conditions", Part 1-3,

Table captions:

Table 1. Specifications of the thrust bearings test rig at GUT laboratory.

Table 2. Test thrust bearings data.

Table 3. Thermocouples locations coordinates.

Table 4. Specifications of the tests.

Table 5. Conditions and results of the steady state tests for front bearing.

Figure captions:

Fig. 1. Thrust bearing test stand used in tests, a) general view of test stand with opened cover of the bearing housing, b) cross section of the housing: 1 – front bearing, 2 – collar, 3 – back bearing, 4 – load piston, 5 – bearing housing, 6 – plate, 7 – torque meter, 8 – distance sensor.

Fig. 2. Torque meter of the thrust bearing test rig, a) general view; b) torque meter idea - schematic diagram; c) result of torque meter calibration carried out before tests, lines represents readings difference of displacement sensors [μm].

Fig. 3. Bearings details: a) pad dimensions, b) view of front bearing mounted in test rig plate.

Fig. 4. Positions and symbols of the temperature sensors installed in the front bearing (same positions were used for back bearing).

Fig. 5. Highest temperature in the front bearing in the steady state tests.

Fig. 6. Steady state tests results: a) friction torque M in the front bearing [Nm]; b) coefficient of friction μ [-].

Fig. 7. Mean film thickness over pad support h [μm].

Fig. 8. Temperature [°C] in the pad A of the front bearing; a) 2.5 MPa, 3000rpm; b) 10 MPa, 100 rpm.

Fig. 9. Results of temperatures [°C] for pad A of the Front Bearing as a function of time (in minutes), START / STOP tests – cycle no 105. Oil supply T_{in} and drain temperature T_{out} [°C], axial force W [kN], shaft speed n (rpm/10 – reduced to fit scale of the graph) are also plotted.

Fig. 10. Results of friction torque (M- Nm) and mean film thickness over the pad support (h - μm) as a function of time from the beginning of the test (in minutes), START / STOP tests –

cycle no 105, axial force W (kN), shaft speed (n- rpm/10 – reduced to fit scale of the graph) are also plotted, a) whole cycle course, b) moment of the shaft stopping.

Fig. 11. Maximum measured temperature (^{o}C) in all pads during individual start / stop tests.

Fig. 12. Results of start / stop tests: a) minimum friction torque (Nm) measured before stop of the shaft during shut-down stage of each individual cycle; b) shaft rotational speed at the moment of minimum friction torque and just before shaft stop for each individual cycle.

Fig. 13. Photographs of the front bearing pad B a) before and b) after START / STOP tests.

Fig. 14. Stribeck curve tests results: a) coefficient of friction [-] as a function of Hersey Number [-], b) minimum distance sensor reading [μm] (corrected with reference value) as a function of Hersey Number [-] (Hs = ηn/p; η – dynamic oil viscosity [Pa s], n – shaft speed [1/s], p – average pressure [Pa]) measured at two levels of axial bearing load.

Fig. 15. Temperatures measured in hottest pad area (75%/75% point) as a function of Hersey Number [-] for all instrumented pads under specific bearings pressure 5.0 MPa.

Table 1.

Parameter	*Value*
Bearing outer diameter	Up to 200 mm
Bearing axial load	Up to 90 kN
Rotational speed of the motor	50-4500 rpm
Lubricating oil flow ($Q_{in\ f} + Q_{in\ b}$)	adjustable, up to 45 l/min

Table 2.

Quantity	*Unit*	*Value*
outer bearing diameter	[mm]	175
inner bearing diameter	[mm]	95
pad thickness	[mm]	14 (16 mm including support)
number of pads	[-]	8
angular length of the pad	[^{o}]	38
pivot type	[-]	linear, symmetric edge
pad material		steel, no bearing alloy layer

Table 3.

Thermocouple symbol	*R_p [-]* *$R_p = R_i / L$* *radial relative coordinate*	*Θ_p [-]* *$\Theta_p = \Theta / \beta$* *tangential relative coordinate*	*z [mm]* *distance from the sliding surface*	*remarks*
TF_A1, TF_B1	0.75	0.25	- 3.0	inlet area
TF_A2, TF_B2	0.75	0.75	-3.0	high temp. area - standard location
TF_A3	0.5	~ 0.75	-3.0	middle of the outlet area
TF_B2b	0.75	0.75	-11.0	pad bottom

Table 4.

Test	*Conditions*		*Remarks*
	specific load	*rotational speed (sliding speed)*	
steady state tests	2.5 MPa	3000 rpm (21.3 m/s)	-
	2.5 and 5 MPa	1000 rpm (7.1 m/s)	-
	2.5, 5 and 10 MPa	100 rpm (0.71 m/s)	test at 10 MPa was carried out with a 4 pad bearing
start stops	0 ↗ 5.6 MPa	0 ↗ 500 rpm ↘ 0 (0 ↗ 3.6 m/s ↘ 0)	start with no load (from 0 to 500 rpm in ~40 s), load was applied up to 80 kN in ~35 s, after steady state operation (~3 minutes) stopping under full load in ~60 s, one start stop test duration ~5 minutes.
transition to mixed friction	2.5 and 5 MPa	120 rpm ↘ 20-25 rpm (0.85 m/s ↘ 0.14-0.18 m/s)	20 rpm for 2.5 MPa 25 rpm for 5 MPa

Table 5.

Parameter	*Unit*	*Test I*	*Test II*	*Test III*	*Test IV*	*Test V*	*Test VI*
n	(rpm)	2998	1000	1000	100	100	100
p	(MPa)	2.5	2.5	5.0	2.5	5.0	10.0*
W	(kN)	35.8	35.8	71.6	35.8	71.6	71.6
TF_A1	(°C)	68.9	57.3	61.9	42.4	43.1	42.6
TF_A2	(°C)	86.2	60.5	65.2	42.4	43.1	42.6
TF_A3	(°C)	85.4	59.9	64.3	42.3	42.9	42.5
TF_B1	(°C)	66.6	57.3	61.9	42.2	42.9	42.4
TF_B2	(°C)	87.4	61.1	66.0	42.3	43.1	42.5
TF_B2b	(°C)	72.2	55.4	58.8	42.0	42.6	42.2
h	(μm)	37.6	26.6	20.6	11.0	8.6	6.6
M	(Nm)	16.8	12.3	16.3	7.0	8.4	6.6
μ	(-)	0.0069	0.0051	0.0034	0.0029	0.0017	0.0014
** because of axial load limitations specific load of 10 MPa was realized in a bearing with 4 pads instead of 8 - every second pad was removed*							

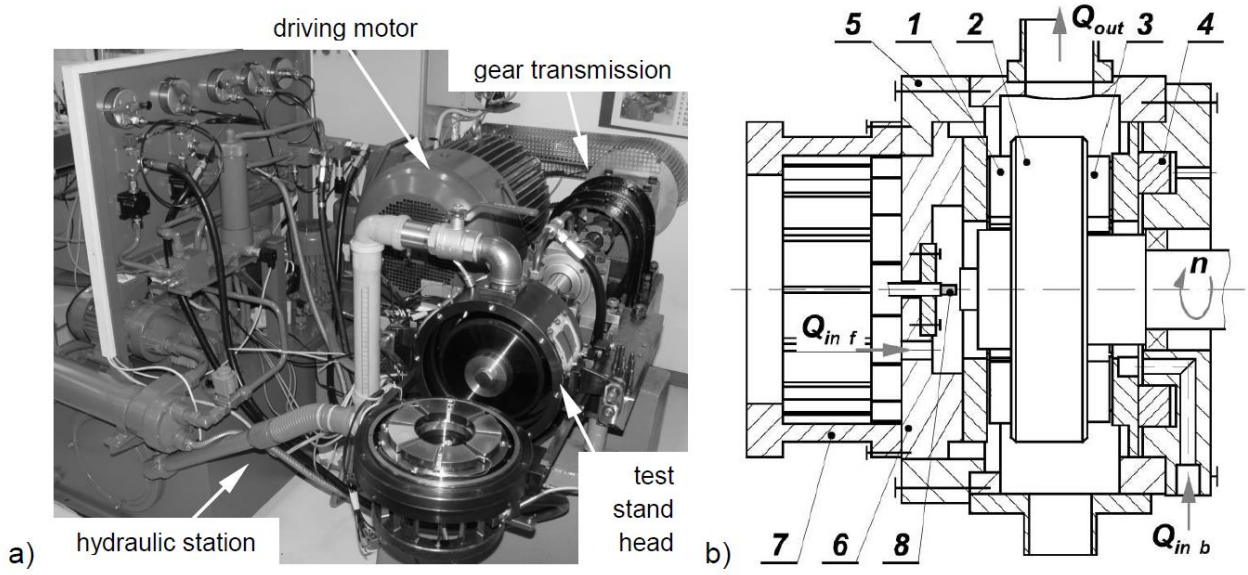

Fig. 1.

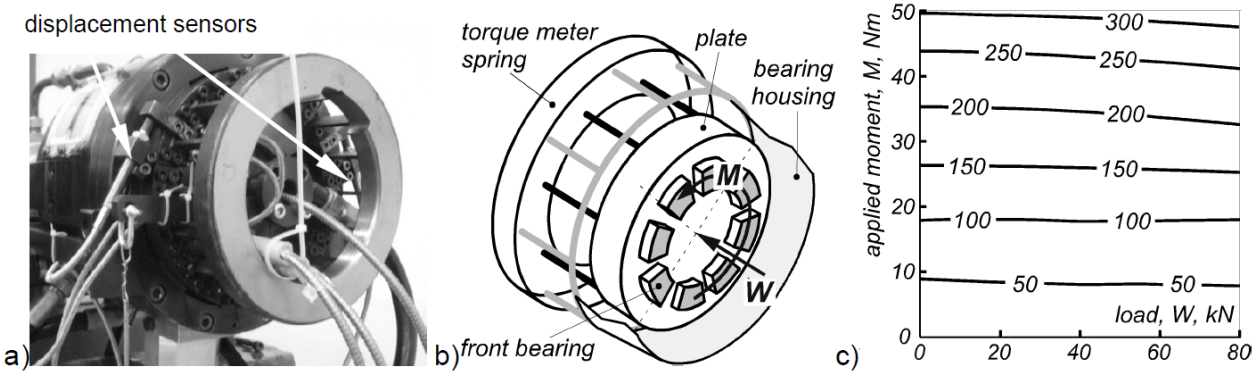

Fig. 2.

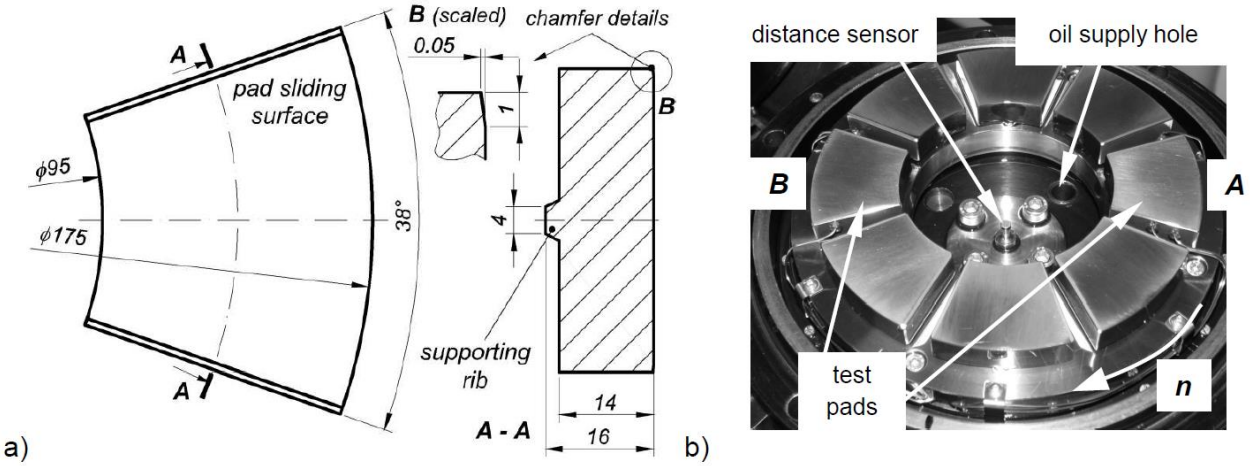

Fig. 3.

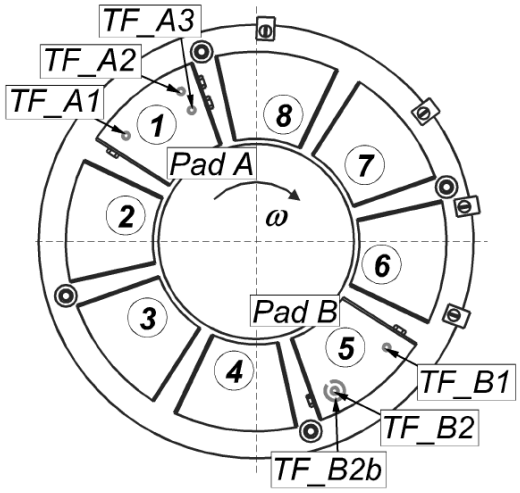

Fig. 4.

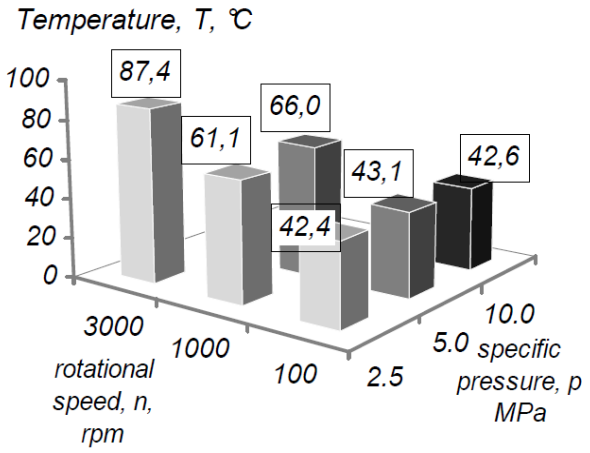

Fig. 5.

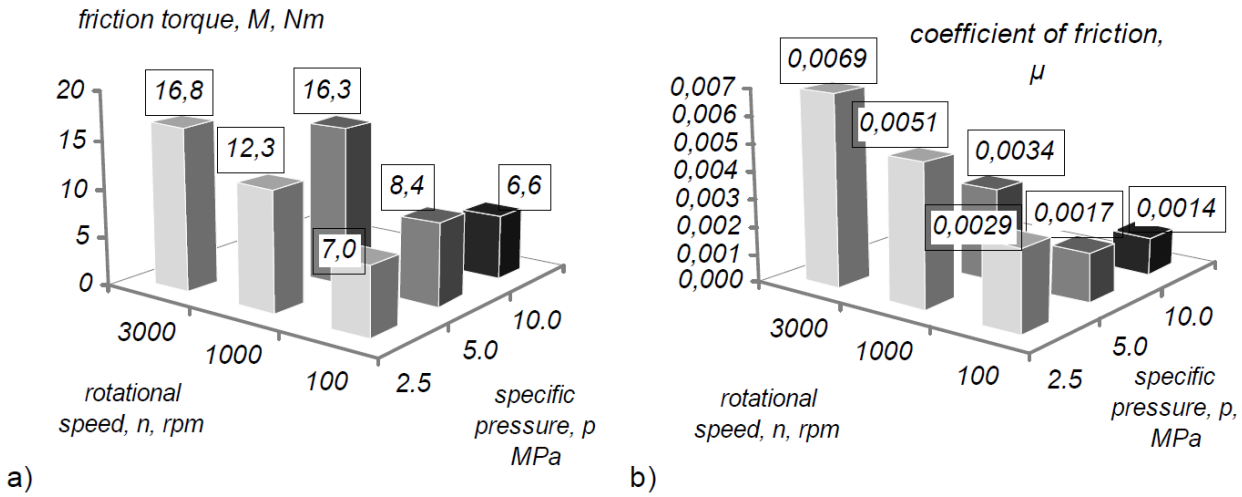

Fig. 6.

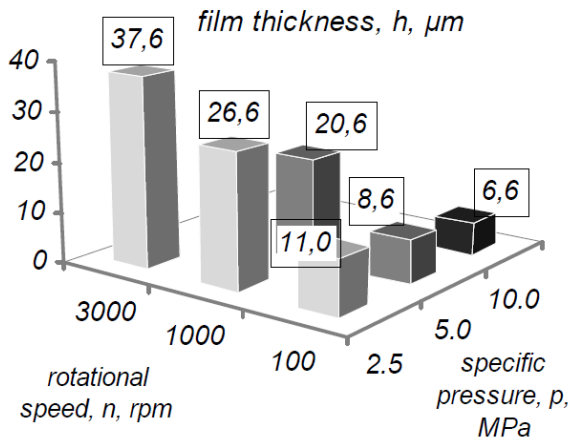

Fig. 7.

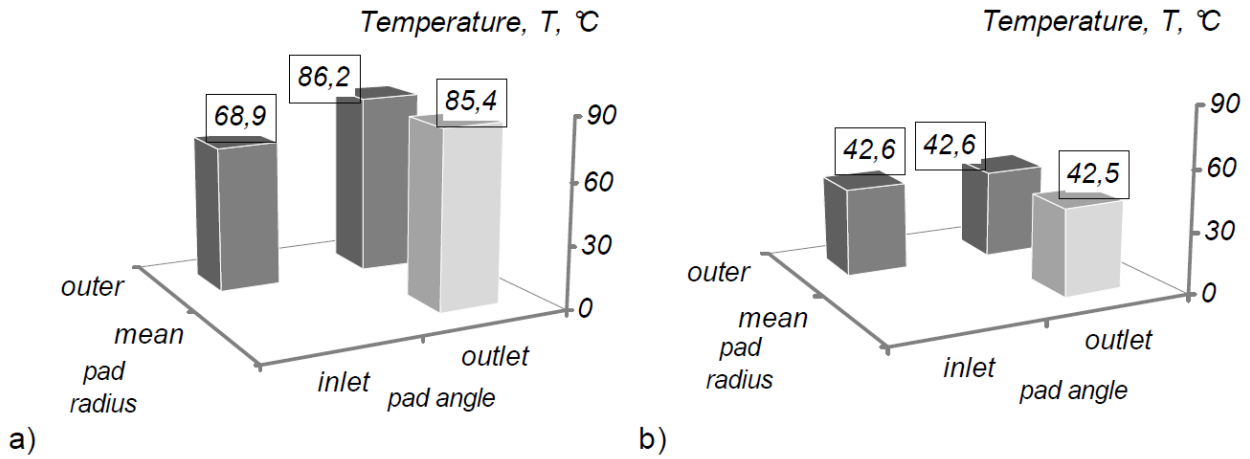

Fig. 8.

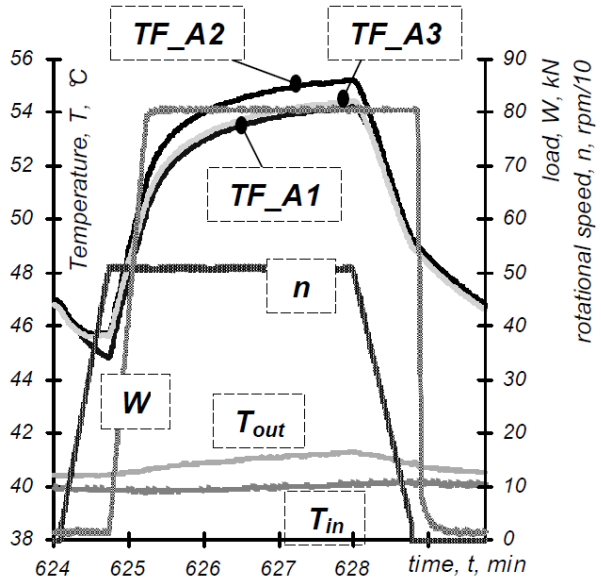

Fig. 9.

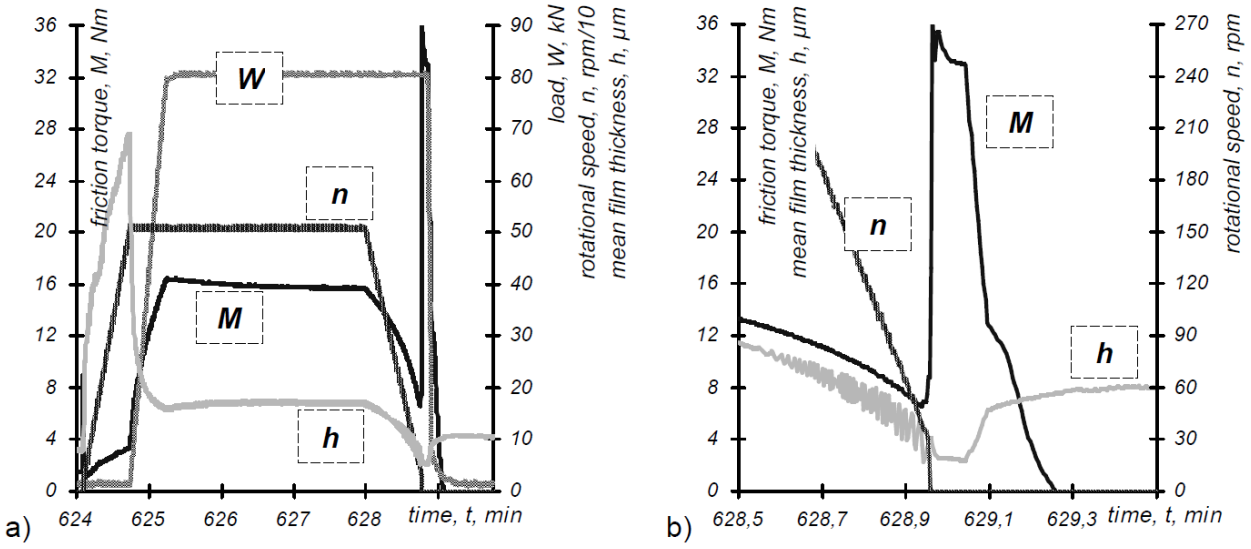

Fig. 10.

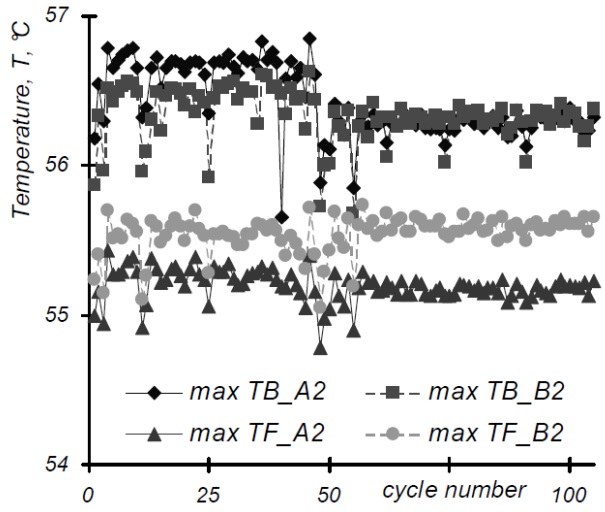

Fig. 11.

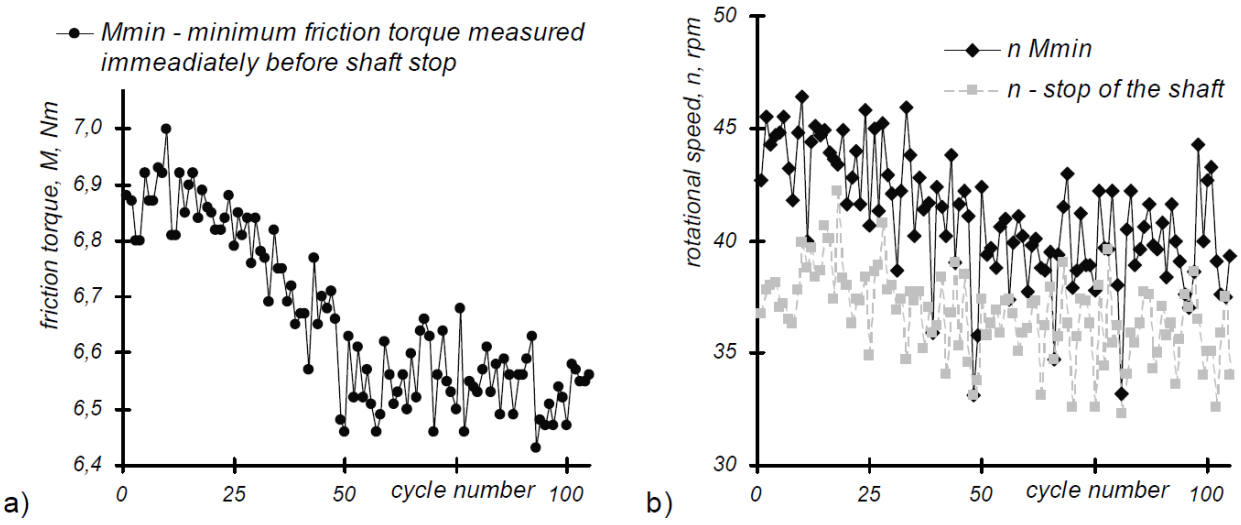

Fig. 12.

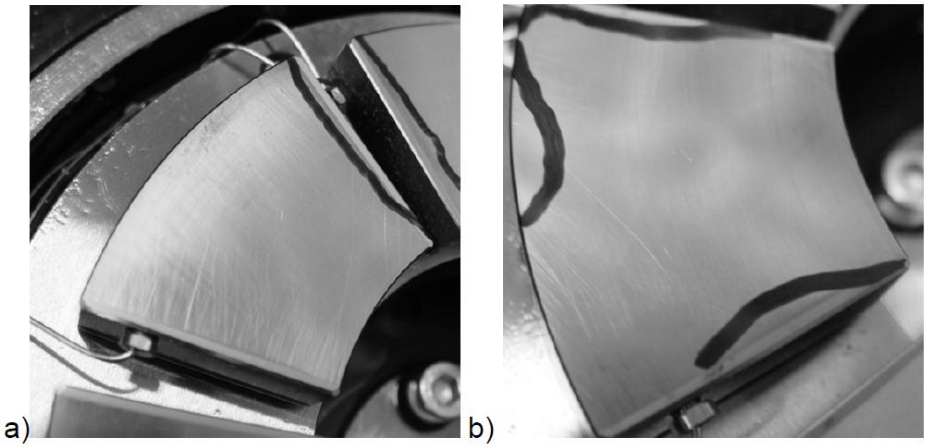

Fig. 13.

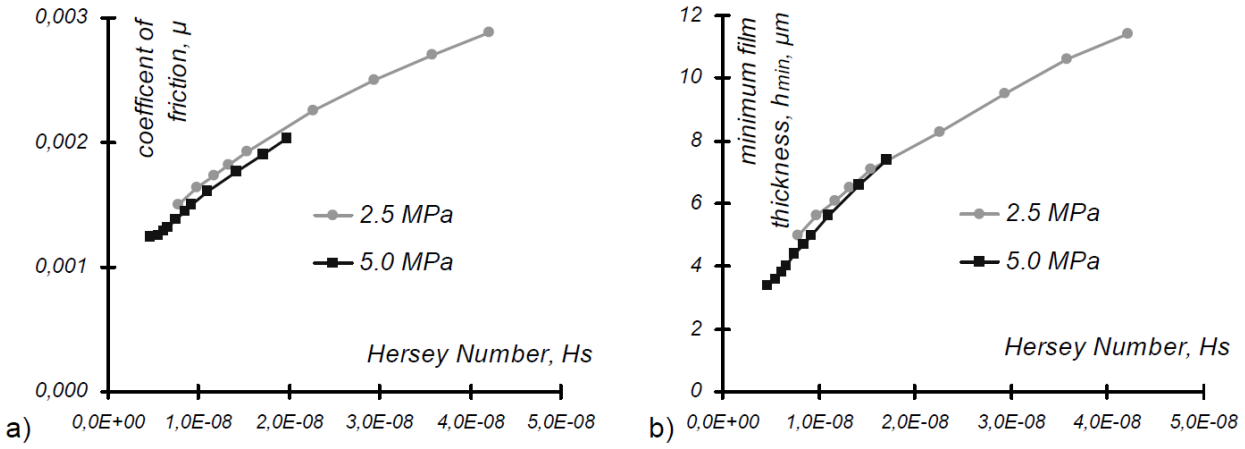

Fig. 14.

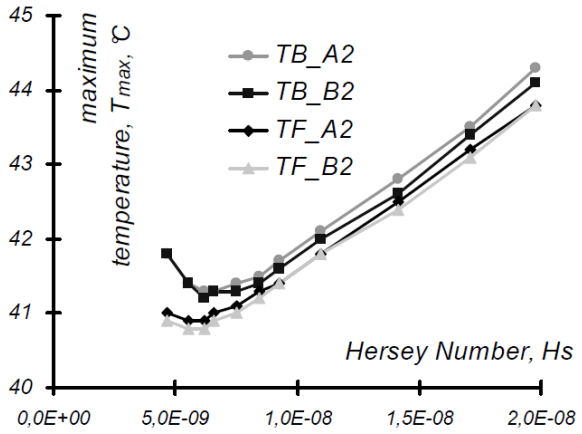

Fig. 15.